ronto, Canada, July 8–13, 1979, Abstr. No. 03-4-S95, p 194.
Dunn, M. F., & Hutchison, J. S. (1973) *Biochemistry 12*, 4882.
Dunn, M. F., & Bernhard, S. A. (1974) *Tech. Chem. (N.Y.) 6 (Part I)*, 665–682.
Dunn, M. F., Biellmann, J.-F., & Branlant, G. (1975) *Biochemistry 14*, 3176.
Dunn, M. F., Schack, P., Koerber, S. C., Au, A. M.-J., Saliman, G., & Morris, R. G. (1977) in *Pyridine Nucleotide-Dependent Dehydrogenase* (Sund, H., Ed.) pp 206–221, Verlag/W. de Gruyter, Berlin.
Dunn, M. F., Bernhard, S. A., Anderson, D., Copeland, A., Morris, R. G., & Roque, J.-P. (1979) *Biochemistry 18*, 2346.
Dworschack, R. T., & Plapp, B. V. (1977) *Biochemistry 16*, 2716.
Jencks, W. P. (1969) *Catalysis in Chemistry and Enzymology*, pp 577–585, McGraw-Hill, New York.
Jencks, W. P. (1972) *Chem. Rev. 72*, 705.
Kvassman, J., & Pettersson, G. (1978) *Eur. J. Biochem. 87*, 417.
McFarland, J. T., & Bernhard, S. A. (1972) *Biochemistry 11*, 1486.
McFarland, J. T., & Chu, Y.-H. (1975) *Biochemistry 14*, 1140.
Rafter, G. W., & Colwick, S. P. (1957) *Methods Enzymol. 3*, 887.
Shore, J. D., Gutfreund, H., Brooks, R. L., Santiago, D., & Santiago, P. (1974) *Biochemistry 13*, 4185.
Silverstein, E. (1965) *Anal. Biochem. 12*, 199.
Sloan, D. L., Young, J. M., & Mildvan, A. S. (1975) *Biochemistry 14*, 1998.
Sund, H., & Theorell, H. (1963) *Enzymes, 2nd Ed. 7*, 25.
Theorell, H., & Yonetani, T. (1963) *Biochem. Z. 338*, 537.

Investigation of a Novel Liver Alcohol Dehydrogenase Catalyzed Redox–Elimination Reaction Involving Arylnitroso Substrate Analogues†

Steven C. Koerber, Poul Schack,‡ Alice M.-J. Au,§ and Michael F. Dunn*

ABSTRACT: The kinetics, product identifications, stoichiometries, and pH dependencies of the reaction of horse liver alcohol dehydrogenase (LADH) with two arylnitroso substrate analogues *p*-nitroso-*N*,*N*-dimethylaniline (NDMA) and *p*-nitroso-*N*-phenylaniline (NPA) are reported. A preliminary account of the reaction with NDMA has been published [Dunn, M. F., & Bernhard, S. A. (1971) *Biochemistry 10*, 4569]. Under conditions of [E(NADH)] ≫ [S], the second-order rate constant for the bleaching of the intense absorbance at 440 nm of both substrates is independent of pH in the range 4–10. NPA shows an apparent diminution in rate above pH 9, but this is attributable to substrate ionization to the nonreactive anion. The rate constants are 6.6×10^7 M^{-1} s^{-1} for NPA and 2.5×10^7 M^{-1} s^{-1} for NDMA. Isolation and derivitization followed by IR, UV, and mass spectral analysis of the product of NPA reduction implicate *N*-phenylbenzoquinonediimine as the immediate enzymatic product. The identification of the immediate enzymatic product of NDMA reduction is complicated by an ensuing nonenzymatic reduction by (excess) NADH, allowing a dismutation equilibrium to generate a previously described transient intermediate [Schack, P., & Dunn, M. F. (1972) paper presented at the 8th Federation of European Biochemical Societies Meeting, Amsterdam, Holland, Aug 1972] now assigned to the radical cation of *N*,*N*-dimethyl-*p*-phenylenediamine. However, a chemical trapping technique using 4-chloro-1-naphthol shows that the *N*,*N*-dimethylbenzoquinonediiminium cation produced is chemically and kinetically competent to be the enzymatic product. A mechanism is proposed to account for the novel reaction of both substrates. Upon substrate binding, coordination of the nitroso oxygen to the active-site zinc activates the nitroso nitrogen for nucleophilic attack by NADH, giving the corresponding zinc-coordinated hydroxylamine and NAD^+ at the active site. Then, the hydroxylamine undergoes rapid hydroxide elimination to form the benzoquinonediimine product. The lack of a kinetic isotope effect when (4*R*)-4-deuterionicotinamide adenine dinucleotide is substituted for NADH in transient experiments argues that these nitroso compounds are unique in that the rate-determining step for the chemical transformation appears to be diffusion to the enzyme active site.

In 1971 Dunn and Bernhard published a preliminary account of the reaction of NADH[1] with the intensely chromophoric substrate analogue *p*-nitroso-*N*,*N*-dimethylaniline (NDMA; λ_{max} 440 nm; ϵ_{440} 3.54×10^4 M^{-1} cm^{-1}) mediated by equine liver alcohol dehydrogenase (EC 1.1.1.1, LADH). Because the optical density changes at 330 nm were found to lag considerably behind those at 440 nm, it was suggested that stoichiometrically significant amounts of a nonenzymatic intermediate were generated in the reaction. A transient species

† From the Department of Biochemistry, University of California, Riverside, Riverside, California 92521. *Received April 3, 1979; revised manuscript received September 10, 1979.* This work was supported in part by National Science Foundation Grants GB 31151 and BMS 75-20339.

‡ Present address: Fysisk-Kemisk Institut, Technical University of Denmark, DTH 206, DK 2800, Lyngby, Denmark.
§ Present address: University of California, San Francisco, School of Medicine, Department of Neurology, San Francisco, CA 94103.

[1] Abbreviations used: DPD, *N*,*N*-dimethyl-*p*-phenylenediamine; LADH or E, horse liver alcohol dehydrogenase (EC 1.1.1.1); NAD^+ and NADH, oxidized and reduced nicotinamide adenine dinucleotide; NADD, (4*R*)-4-deuterionicotinamide adenine dinucleotide; NDMA, *p*-nitroso-*N*,*N*-dimethylaniline; NPA, *p*-nitroso-*N*-phenylaniline; 4-CN, 4-chloro-1-naphthol; S, substrate; RNO, arylnitroso substrate analogue; QDI^+, quinonediiminium ion; QDI, quinonediimine.

0006-2960/80/0419-0731$01.00/0

absorbing in the range 510–600 nm was subsequently found to have the kinetic properties of the assumed intermediate (Schack & Dunn, 1972; Dunn et al., 1977).

The present work reexamines and extends the scope of the original report and includes a detailed study of the LADH-catalyzed reaction of NADH with *p*-nitroso-*N*-phenylaniline (NPA), an interesting homologue of NDMA. It will be shown

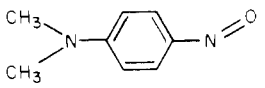

NDMA

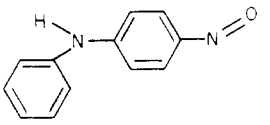

NPA

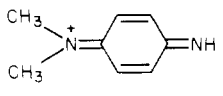

QDI^+

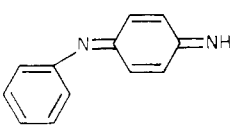

I

that LADH catalyzes novel redox–elimination reactions converting these arylnitroso compounds to the corresponding benzoquinonediiminium cation (QDI^+) and the benzoquinonediimine (compound I), respectively. The results of these studies are fully consistent with the involvement of zinc ion as a Lewis acid catalyst in the activation of substrate for reaction with bound NADH during the chemical transformation.

Experimental Section

Materials

Horse liver alcohol dehydrogenase (Boehringer Mannheim Biochemicals) was further purified by the method of Dunn & Hutchison (1973). Active-site concentrations were determined by the NAD^+–pyrazole spectrophotometric assay of Theorell & Yonetani (1963) and are reported throughout as N, the normality.

The coenzymes NAD^+ and NADH (Sigma Chemical Co. grades V and III, respectively) were used without further purification in all experiments except those involving deuterium isotope effects (see Methods). Both specifically labeled (4*R*)-4-deuterionicotinamide adenine dinucleotide (NADD) and isotopically normal NADH were synthesized and isolated by the method of Rafter & Colwick (1957) modified according to the method of Dunn & Hutchison (1973). The crude products were further purified by the method of Silverstein (1965).

N,*N*-Dimethyl-*p*-phenylenediamine (DPD) and NDMA (Eastman) were used without further purification. NPA (Aldrich) was purified by vacuum sublimation, and the concentrations of stock solutions were determined spectrophotometrically (λ_{max} 440 nm; ϵ_{max} 3.30×10^4 M^{-1} cm^{-1}). 4-Chloro-1-naphthol (4-CN) was obtained from Aldrich and used without further purification. Reagent-grade buffer salts, acetonitrile, and acetic anhydride were obtained from standard chemical suppliers and were used without further purification. Buffer solutions were prepared with doubly distilled water and kept chloride ion free.

Methods

Spectral and Kinetic Measurements. All static UV–visible spectroscopy was performed with a Varian Model 635 spectrophotometer thermostated at 25.0 ± 0.2 °C. Transient kinetic studies were performed with a Durrum Model D-110 stopped-flow spectrophotometer (20-mm light path; dead time ~3.0 ms) which is interfaced for on-line computer data acquisition and analysis. The hardware and software for this system have been described by Dunn et al. (1979). The concentrations reported refer to conditions after mixing. The OD values reported have been corrected to the values expected for a 1-cm light path.

Product Isolation and Identification. The LADH catalyzed reaction of NPA with NADH was carried out on a preparative scale by mixing 120 nmol of LADH with 90 μmol of NADH and 90 μmol of NPA in aqueous 0.1 M sodium pyrophosphate, pH 8.75 (final volume 6.5 mL). Gel filtration of the final reaction mixture (Sephadex G-15, 1.25×25 cm^3) gave a clean separation of three components: enzyme, coenzyme, and a product derived from NPA (compound I; λ_{max} 420 nm).

Compound I was found to undergo spontaneous (i.e., nonenzymatic) transformation to a new chromophoric species, compound II (λ_{max} 440 nm; $t_{1/2}$ ~20 min). Attempts to isolate I by extraction into organic solvents and evaporation at ambient temperature invariably resulted in the isolation of II. Treatment of I with acetic anhydride was found to accelerate the transformation of I to II. Due to the labile nature of I, no further attempts at its isolation were made. Isolation and purification of II via $CHCl_3$ extraction, evaporation, and sublimation (50 μHg, 25 °C) gave II as an orange, crystalline solid. Treatment of I with $NaBH_4$ followed by acetic anhydride gave compound III. The IR spectrum of II (in $CHCl_3$) exhibits characteristic absorptions at $\bar{\nu}$ = 1626, 1616, 1317, 1088, and 869 cm^{-1}; no absorptions were detected in the range 2500–4000 cm^{-1}. The mass spectrum of II exhibits intense peaks at *m*/*e* values of 183, 154, 129, 103, and 77. A comparison of these three types of spectra shows II to be identical with an authentic sample of *N*-phenyl-*p*-benzoquinonemonoimine, prepared by careful oxidation of *p*-hydroxyaniline with Tollins' reagent (Shriner et al., 1959). III exhibits a UV absorption with λ_{max} 283 nm in aqueous sodium pyrophosphate buffer, pH 8.75. The IR spectrum of III (in $CHCl_3$) exhibits characteristic absorbances at 3450, 1682, 1517, and 1300 cm^{-1}. The mass spectrum of III yields intense peaks at *m*/*e* values of 226 and 184. A comparison of these three types of spectra shows III to be identical with an authentic sample of *N*-acetyl-*N'*-phenyl-*p*-phenylenediamine (prepared by the acetylation of *N*-phenyl-*p*-phenylenediamine with acetic anhydride).

The final products from the LADH catalyzed reaction of NDMA with NADH were generated on a preparative scale by mixing 120 μmol of NDMA with 200 nmol of LADH (normal), 122 μmol of NADH, and 28 mmol of ethanol in aqueous 0.1 M sodium pyrosphosphate, pH 8.75. The product mixture was neutralized with Na_2CO_3, mixed with 120 mmol of acetic anhydride and extracted with $CHCl_3$. The organic phase was evaporated to a small volume and subjected to TLC on 0.5-mm thick silica G plates developed in CH_3CN. Of the five bands which appeared, the major band migrated with an R_f = 0.56 as did an authentic sample of *N*-acetyl-DPD.

The IR spectrum of this major band (in KBr pellet) shows characteristic peaks at $\bar{\nu}$ = 3310, 3260, 1460, 1520, and 806 cm^{-1}. Its mass spectrum exhibits intense peaks at *m*/*e* values of 178, 136, 135, 121, 77, 65, and 43. A comparison of these spectra shows the major band to be identical with that of an authentic sample of *N*-acetyl-DPD, prepared by acetylation of DPD with acetic anhydride. It was concluded that the remaining four bands on the TLC plate are derived from air oxidation, hydrolysis, and deamination of the labile DPD prior to acetylation.

As will be shown, the enzymatic product almost certainly is the *N*,*N*-dimethyl-*p*-benzoquinonediiminium ion (QDI^+).

Consequently, a more direct chemical technique suited to stopped-flow methodology was employed to trap this product. 4-Chloro-1-naphthol (4-CN) has been shown by Tong & Glesmann (1957) to undergo oxidative condensation with QDI^+, resulting in the elimination of HCl and the formation of a characteristic dye with a broad, intense maximum at ~600 nm:

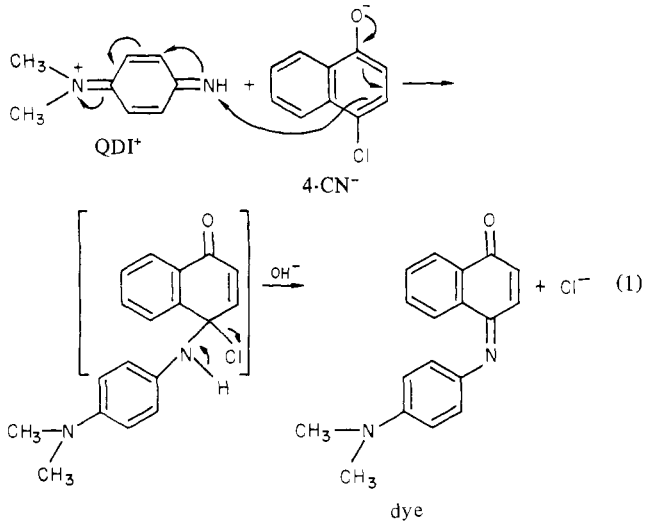

(1)

Tong and Glesmann have found the kinetic expression for this reaction to be

$$\frac{d[\text{dye}]}{dt} = k[\text{4-CN}^-][\text{QDI}^+] \qquad (2)$$

where 4-CN^- is the 4-chloro-1-naphthoxide ion. The second-order rate constant, k, for this reaction is $\sim 1.0 \times 10^6$ M^{-1} s^{-1} (Tong & Glesmann, 1957). Due to the ionization of 4-CN to 4-CN^- (with $pK = 8.65$), the solubility of 4-CN is pH dependent. Consequently, all kinetic studies using 4-CN were at pH values above pH 9.

The stoichiometry of the NADH/NDMA reaction was measured spectrophotometrically under single turnover conditions (i.e., [pyrazole] ≫ [NADH] ≫ [NDMA] > [E]) by noting the change in optical density at 330 nm upon addition of NDMA to the LADH(NADH) complex. McFarland & Bernhard (1972) and Dunn et al. (1979) have shown that the LADH-catalyzed reduction of aldehydes is limited to a single turnover of sites in the presence of concentrated (i.e., 20 mM) pyrazole by the essentially irreversible formation of an E-(NAD^+,pyrazole) ternary complex. The corrections necessary for this determination arise from the overlap of the NADH spectrum with that of NDMA and E(NAD,pyrazole). The correction for the NADH contribution was calculated by assuming that all LADH sites turned over only once. The correction for the E(NAD,pyrazole) contribution was calculated by assuming its absorbance at 330 nm to be ~13% of the E(NADH) absorbance after Theorell & Yonetani (1963) and Dunn et al. (1979). The stoichiometry of the NADH/NPA reaction was determined in a similar fashion.

Isotope and pH Effects. Deuterium isotope effects were determined for the reaction of NPA (at pH 7) and NDMA (at pH 8.75) under single turnover conditions (i.e., [NADX] > [E] > [S], where NADX is either NADH or NADD), by following the disappearance of these substrates at 440 nm.

Prolonged exposure to extremes of pH gradually degrades the LADH(NADH) binary complex; LADH loses zinc ion above pH 10 (DeTraglia et al., 1977), whereas NADH is subject to a general acid catalyzed decomposition (Alivisatos et al., 1965). Consequently, pH studies employed a "pH-jump" technique wherein LADH and NADH weakly buffered in one syringe are mixed with a strongly buffered substrate solution at a selected pH to give the desired final pH on mixing.

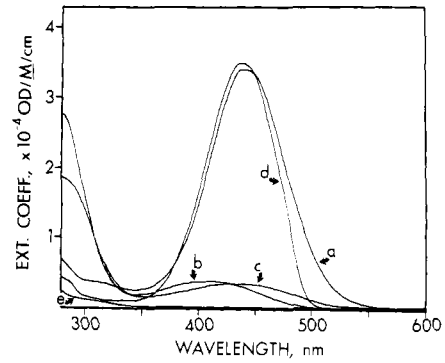

FIGURE 1: Spectra of NPA (a), compound I (b), compound II (c), NDMA (d), and the final product of the NDMA reaction (e) measured in 0.1 M sodium pyrophosphate, pH 8.75, 25 °C.

Results

Final Product Identification and Stoichiometries. The LADH-catalyzed reaction of NADH with NPA gives an initial product (compound I) with λ_{max} 420 nm (see Figure 1). This relatively low energy π–π^* transition indicates I has an extensively delocalized π-electron network; hence, a simple reduction of NPA to the corresponding *N*-arylhydroxylamine would be inconsistent with this finding. Compound I undergoes a spontaneous (nonenzymatic) conversion to II (λ_{max} 440 nm). Compound II is identified as *N*-phenyl-*p*-benzoquinonemonoimine on the basis of IR, UV–visible, and mass spectral comparisons with an authentic sample (see Experimental Section). Treatment of I with $NaBH_4$ followed by acetic anhydride yields compound III (see Experimental Section). Comparison of IR, UV, and mass spectra for III with an authentic sample of *N*-acetyl-*N'*-phenyl-*p*-phenylenediamine shows those compounds to be identical. As indicated by the reappearance of the intense 440-nm absorption band, treatment of I with hydroxylamine regenerates NPA.

The coenzyme product was isolated by molecular sieve chromatography (see Experimental Section) and identified as NAD^+ by the following observations: (a) it functioned quantitatively in the LADH-catalyzed oxidation of ethanol—a reaction noted for its high specificity for NAD^+ (Sund & Theorell, 1963; Anderson & Kaplan, 1959; Cornforth et al., 1963); (b) the UV spectrum of the product and the spectrum of its reduced form are identical with the spectra of authentic samples of NAD^+ and NADH, respectively. The yield of NAD^+ was estimated to be >90% of the theoretical amount expected for the conversion of 1 mol of NADH to NAD^+ for every mole of NPA reduced. These results are summarized in Scheme I.

For purposes of clarity, compound I is shown here as *N*-phenylbenzoquinonediimine. Arguments in support of this structural assignment are presented under Discussion.

The LADH-catalyzed reaction of NADH with NDMA is a more complicated reaction. As will be discussed in detail in subsequent sections, the appearance of the final reaction product is preceded by the appearance and decay of an intermediate absorbing at 555 nm. The appearance of this intermediate lags behind the disappearance of NDMA. The final reaction product (after acetylation with acetic anhydride, Scheme II) shows IR, UV, and mass spectra that are identical with the corresponding spectra for *N*-acetyl-DPD. Dunn &

Scheme I

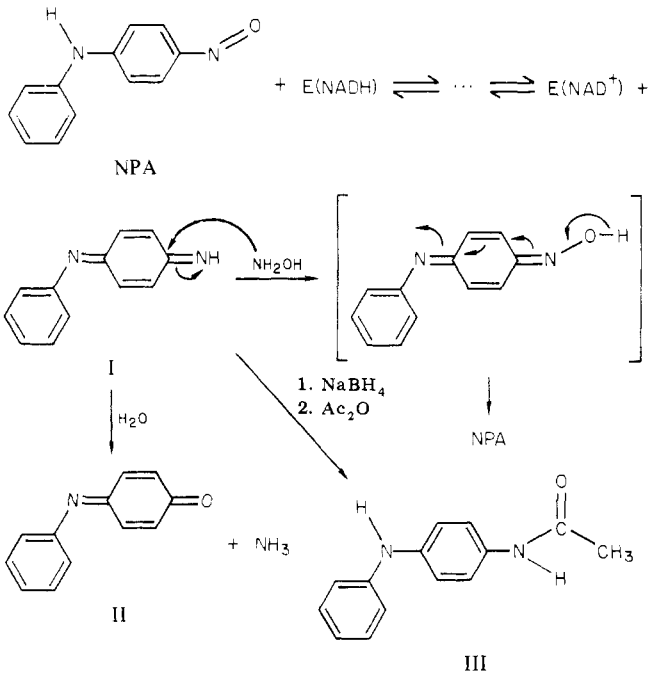

Scheme II

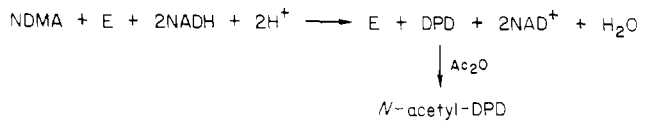

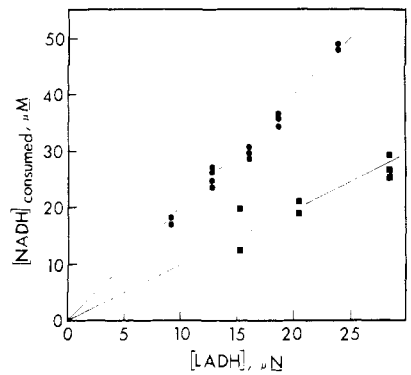

FIGURE 2: Stoichiometric relation of NADH consumed in a single turnover of NPA (boxes) and NDMA (circles). Conditions: [NPA] = 10.0 μM; [NDMA] = 10.0 μM; [NADH] = 0.234 mM; [pyrazole] = 20.0 mM; pH 8.75, 0.1 M sodium pyrophosphate, 25 °C. The determination of Δ[NADH] is described in the text. The straight lines represent theoretical stoichiometries of 1:1 and 2:1.

Bernhard (1971) established that NAD^+ is the coenzyme product of this reaction.

The data presented in Figure 2 establish the stoichiometries of the NPA and NDMA reactions. In the presence of excess NADH, the NDMA reaction occurs with the conversion of two NADH molecules to NAD^+ for each molecule of NDMA consumed (Scheme II), whereas only one NADH molecule is oxidized for each molecule of NPA comsumed (viz., the first step in Scheme I).

General Kinetic Properties. When the concentration of NADH-saturated sites is in excess, the time course for disappearance of either substrate (measured at 440 nm; see Figure 1) is characterized by a rapid (apparent first-order) disappearance (Figures 2–4). Under conditions of steady-state saturation by NADH and either substrate, the magnitude of k_{cat} at pH 8.75 (10 ± 2.5 s^{-1}) is numerically similar to the rate

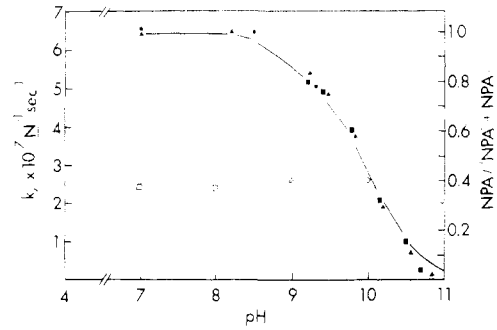

FIGURE 3: Bimolecular rate constants of NPA (■, ●) and NDMA (△, □, ○, ◇) reacting with LADH as a function of pH. Each datum represents the slope of the apparent rate of decay of substrate vs. [LADH] under the conditions [NADH] > [E] > [S]. LADH and NADH were preincubated in one syringe in 10 mM sodium pyrophosphate, pH 8.75. The buffers for the other syringe were as follows: (○) 0.2 M acetate; (□) 0.1 M phosphate; (△) 0.2 M pyrophosphate; (◇) 0.2 M carbonate; (●) (below pH 8) 0.1 M phosphate; (●) (above pH 8) 0.1 M pyrophosphate; (■) 0.1 M carbonate; (▲) represent values of NPA/(NPA$^-$ + NPA) (right-hand ordinate) calculated from the pH dependence of the spectrum of NPA. The solid line is the theoretical curve predicted for a single protonic ionization with pK = 9.8.

of NAD^+ desorption from the enzyme (DeTraglia et al., 1977). The dependence of the initial velocity of disappearance of either substrate under steady-state conditions at pH 8.75 adheres to the Michaelis–Menten equation and yields apparent K_m values of 4.1 × 10^{-7} M for NPA and 5.1 × 10^{-7} M for NDMA.

Transient Kinetic Properties and pH Dependencies. The disappearance of NPA at 440 nm under single turnover conditions (i.e., [E(NADH)] > [NPA]), is well fit by a single exponential decay. The apparent first-order rate constants are directly proportional to the coenzyme-saturated enzyme site concentration with an apparent second-order rate constant of 6.6 × 10^7 M^{-1} s^{-1} in the pH region 7–8.5. Above pH 8.5, the apparent second-order rate constant for NPA reduction decreases and fits the theoretical curve predicted for a process dependent on a single (preequilibrium) protonic ionization with pK_a = 9.8 (see Figure 3). The spectrum of NPA shows a similar pH dependence over this same pH range with pK_a = 9.8. The coincidence of these two pH transitions demonstrates that the ionization of NPA (eq 3) accounts for the dependence of rate on pH.

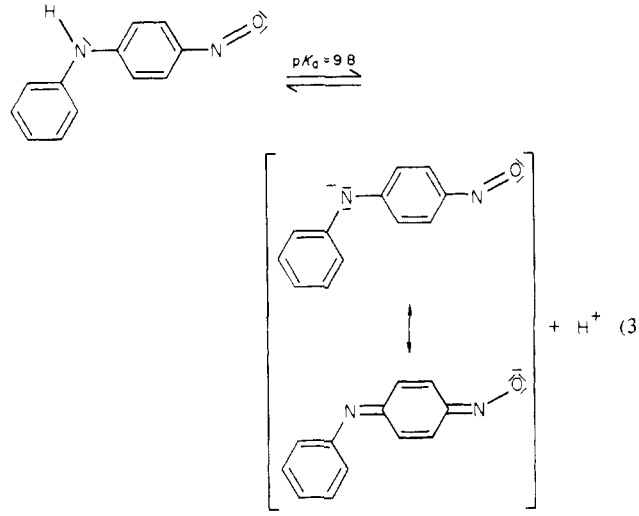

The disappearance of NDMA measured at 440 nm under single turnover conditions is similarly well fit by a single exponential decay. The apparent first-order rate constants are

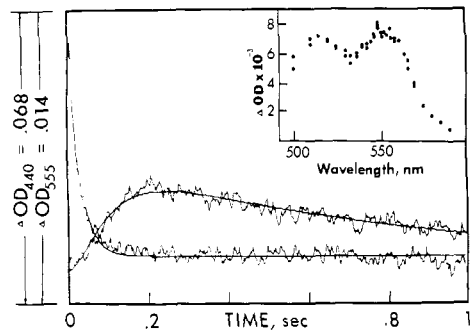

FIGURE 4: Time courses at 440 and 555 nm for the NDMA reaction. Conditions: [E] = 1.94 μN; [pyrazole] = 20.0 mM; 0.1 M sodium pyrophosphate, pH 8.75. Note the different full-scale ordinate values for the two time courses. Inset: the "reconstructed" spectrum of the intermediate in the reaction of NDMA with E(NADH). Conditions: [E] = 2 μN; [NADH] = 0.2 mM; [NDMA] = 20 μM; [pyrazole] = 20 mM; 0.1 M sodium pyrophosphate, pH 8.75, 25.2 °C. The protocol for determining optical density changes is described in the text.

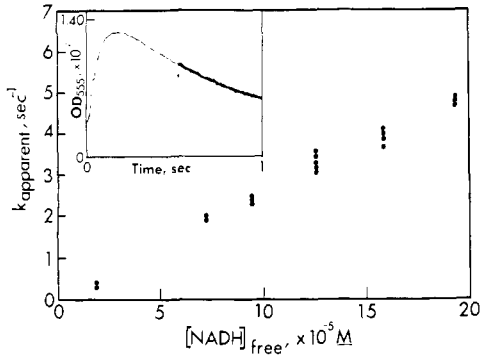

FIGURE 5: Apparent rate of decay of the NDMA intermediate as a function of free NADH. Conditions: [E] = 5 μN; [NDMA] = 0.103 mM; [pyrazole] = 20 mM; [NADH] as shown on the graph; 0.1 M sodium pyrophosphate, pH 8.75, 25 °C. Inset: a typical time course at 555 nm. The darkened portion (indicated with an arrow) represents the part used to calculate the apparent rate of decay, as described in the text.

directly proportional to the coenzyme-saturated enzyme site concentration with an apparent second-order rate constant of $\sim 2.5 \times 10^7$ N^{-1} s^{-1}. The apparent second-order rate constant for NDMA reduction was also determined in the pH range 4–11. As shown in Figure 3, this pH–rate profile is essentially independent of pH.

The kinetic isotope effect on the transient reduction of both substrates was studied under saturating substrate conditions (i.e., [NADX] ≫ [RNO] > [E]) in the presence of 20 mM pyrazole. Neither substrate showed any diminution of rate of decay upon the substitution of deuterium in NADH.

The appearance of a nonenzymatic transient in the reaction of NDMA with the E(NADH) complex absorbing at ~555 nm was first reported by Schack & Dunn (1972). Formation of this intermediate (Figure 4) is characterized by a pronounced lag phase. The intermediate decays in an apparent first-order process (viz., Figure 5). The disappearance of NDMA is nearly complete before any of the 555-nm transient has appeared.

The spectrum of the intermediate for the wavelength range 510–600 nm (shown in the inset to Figure 4) was obtained by measuring the amplitude at the maximum in the time course for intermediate formation and decay as a function of wavelength. Determination of the spectrum at pH 6.8 (not shown) gives the same relative intensities for the peaks at 515 and 555 nm. Hence, the double peak is not the result of a protonation ionization equilibrium. Over this wavelength region, the reconstructed spectrum appears identical with the spectrum of the radical cation of DPD, viz.

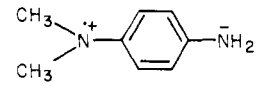

DPD radical cation

which was first described by Michaelis et al. (1939). The work of Baetzold & Tong (1971) establishes that a readily reversible dismutation equilibrium exists wherein 1 mol each of DPD and QDI^+ undergoes a one-electron transfer to generate 2 mol of the radical cation:

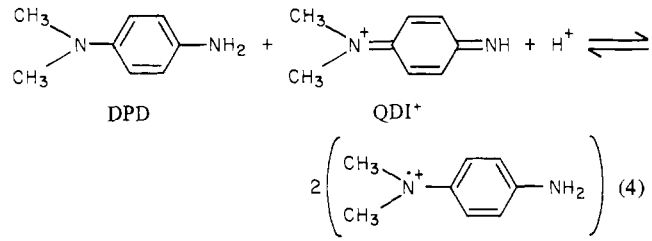

DPD QDI^+

(4)

Since the stoichiometry of NADH consumption is two NADH's per NDMA, the effect of the concentration of free NADH on the apparent rate of decay of the intermediate was investigated. Decay rates were determined by truncating the data to remove the lag phase and appearance of the intermediate. Analysis of the remainder of the time course (the decay phase) gave good fits to an apparent first-order rate law (as shown in the inset to Figure 5). In the presence of 20 mM pyrazole, under conditions of [NDMA] ≫ [LADH] with [E] variable, the effect of free NADH (i.e., $[NADH]_{total} - [E(NADH)]$) on the apparent rate of decay is illustrated in Figure 5. Note that the apparent first-order rate constant for the decay process is proportional to the concentration of free NADH. A plot of log k vs. log $[NADH]_{free}$ (not shown) is linear; the slope of the resultant line has a value of 1, indicating a molecularity of unity for NADH in the decay process. Further, when NADD is substituted for NADH, the apparent rate of decay is subject to an apparent kinetic isotope effect of 1.37 ± 0.16. Correction of this value neglecting secondary isotope effects and assuming approximately equal probabilities for hydride abstraction from the R and S faces of the 1,4-dihydronicotinamide ring gives a statistically corrected kinetic isotope effect (k^H/k^D) of approximately 2.2.

Reaction of 4-CN with NDMA. At alkaline pH, the enzymatic product of the NDMA reaction in the presence of 4-CN^- undergoes a rapid, nonenzymatic reaction to a characteristic blue dye (see Experimental Section). The spectrum of this dye overlaps that of NDMA, and, as shown in Figure 6, an apparent isosbestic point is obtained at 489 nm under conditions of [4-CN] > [NDMA] ≫ [NADH] > [LADH]. Note that ethanol is present in the experiment to recycle the trace of NAD^+ produced back to NADH. As judged by a lack of change in the UV–visible spectral properties of these compounds, 4-CN, NADH, and NDMA do not react in the absence of LADH.

Time courses demonstrating the concurrent disappearance of NDMA and the appearance of dye under saturating 4-CN conditions in the absence of ethanol are shown in the inset to Figure 6.

The apparent first-order rate constants for the change in OD at 440 nm were measured under conditions where [4-CN] and [LADH] are varied and [LADH] and [NADH] > [NDMA]. In accord with a presumed competition between NDMA and 4-CN for the substrate binding site, the apparent second-order rate constant for the disappearance of NDMA

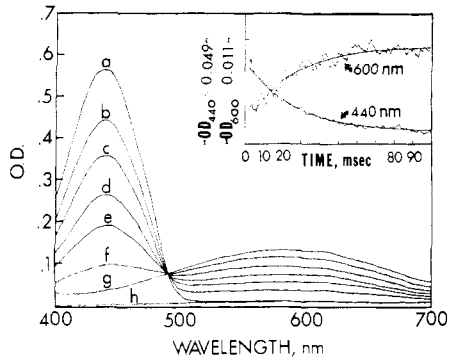

FIGURE 6: Spectra of the NDMA–4-CN system as a function of the extent of reaction with LADH. Conditions: [NDMA] = 17.0 μM; [E] = 0.45 μN; [NADH] = 0.35 μM; [ethanol] = 0.835 mM; [4-CN] = 26.1 μM; 0.1 M sodium carbonate, pH 9.55, 25.0 ± 0.2 °C. Concentrated pyrazole (to give 20 mM) was added at varying times to stop the reaction and to obtain these spectra: (a) 0 s; (b) 30 s; (c) 60 s; (d) 90 s; (e) 120 s; (f) 150 s; (g) 240 s; (h) base line. Inset: transient time courses at 440 and 600 nm. Conditions: [E] = 6.91 μN; [NDMA] = 1.02 μM; [NADH] = 47.1 μM; [4-CN] = 0.238 mM; same buffer conditions as described above. The arrow indicates where the flow was stopped.

(i.e., $k_{app} = k$[LADH]) was found to decrease with increasing concentration of [4-CN].

Discussion

Nature of the Enzymatic Products. The following observations all lead to the conclusion that compound I, the initial product of the LADH-catalyzed reaction of NADH with NPA, is the corresponding *benzoquinonediimine* (viz., Scheme I): (a) the observed long-wavelength absorption at 420 nm suggests that the initial product has an extensively delocalized π-electron network, consistent with the proposed benzoquinonediimine structure; (b) the product undergoes slow nonenzymatic conversion to the benzoquinonemonoimine, compound II; (c) treatment of the initial product with $NaBH_4$ followed by treatment with acetic anhydride yields *N*-acetyl-*N'*-phenyl-*p*-phenylenediamine, compound III; (d) treatment of the initial product with hydroxylamine regenerates NPA.

The identification of the *immediate* product of NDMA reaction as QDI^+ is complicated by the ensuing nonenzymatic conversion to the transient, radical cation of DPD (absorbing between 510 and 600 nm; see the inset of Figure 4) and finally DPD. However, the trapping of QDI^+ by reaction with 4-CN to give the conjugated 1-naphthylphenylenediamine dye provides strong circumstantial evidence that the *immediate* enzymatic product from the NDMA reaction is the corresponding *benzoquinonediiminium cation* (QDI^+; viz., eq 4).

The role of free NADH in the formation and decay of QDI^+ and the DPD radical cation is explained as shown in Scheme III. NADH reduces QDI^+ to DPD, which then reacts with more QDI^+ in a fascile one electron transfer dismutation reaction to produce the radical cation. Scheme III predicts that if there is sufficient NADH present, eventually all of the QDI^+ produced will be reduced to DPD. The dismutation reaction has been carefully documented by Baetzold & Tong (1971).

Nature of the Catalytic Events. The identification of the enzymatic products of both reactions as the corresponding benzoquinonediimines and NAD^+, together with the observed stoichiometric relationships, suggests that the most plausible mechanism for these novel redox–elimination reactions is as shown in Scheme IV. Coordination of the nitroso oxygen to the active-site zinc activates the nitroso nitrogen for nucleophilic attack (i.e., "hydride" transfer) by NADH, giving the

Scheme III

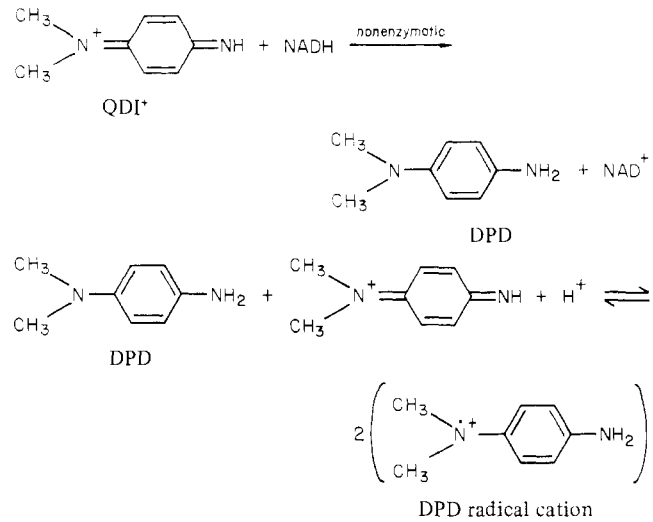

corresponding zinc-coordinated hydroxylamine and NAD^+ at the active site. Then, the hydroxylamine undergoes rapid-elimination of the hydroxyl moiety to form the benzoquinonediimine product and the $E(Zn^{2+}\cdots OH^-,NAD^+)$ complex.[2]

Nature of the LADH(NADH,RNO) Ternary Complex. Under steady-state conditions, the initial velocities of disappearance of both substrates at pH 8.75 saturate with Michaelis constants of 4.1×10^{-7} M for NPA and 5.1×10^{-7} M for NDMA. However, the rate of transient disappearance of both substrates shows no tendency to saturate at [E(NADH)] > 10 μN (i.e., at concentrations of RNO and LADH yielding a k_{app} of $\sim 400\ s^{-1}$) (Dunn & Bernhard, 1971). This can be interpreted as $K_s \gg K_m$ and/or that K_m is dominated by rate terms representing events subsequent to the combination of enzyme and substrate. The second-order rate constant for substrate decay obtained from transient data (see Figure 3) is $2.5 \times 10^7\ N^{-1}\ s^{-1}$ for NDMA and $6.6 \times 10^7\ N^{-1}\ s^{-1}$ for NPA (below pH 9).

If it is assumed that these substrates form inner-sphere complexes with the active-site zinc ion during catalysis as has been shown for other substrates (Morris et al., 1980; Plapp et al., 1978; Brändén et al., 1979), then a more detailed interpretation of these kinetic observations is possible. Previous work from this laboratory (Dunn & Hutchison, 1973; Dunn et al., 1975; Morris et al., 1980) documents an obligatory intermediate in the reaction of the E(NADH) complex with *trans*-4-(*N*,*N*-dimethylamino)cinnamaldehyde (DACA). The spectral and kinetic properties of this intermediate and the 3.7-Å resolution X-ray structure (Brändén et al., 1979; J.-P. Sarmama and E. Zeppezauer, private communication) are fully consistent with direct coordination of the active-site zinc

[2] Arylhydroxylamines are known to undergo iminium ion formation and rearrangement via a specific hydronium ion catalyzed reaction. *N*-Phenylhydroxylamine undergoes an acid-catalyzed rearrangement to *o*- and *p*-hydroxyaniline via a delocalized iminium ion intermediate (Bamberger, 1894; Heller et al., 1951). A nonenzymatic, specific hydronium ion catalyzed pathway could be proposed as an alternative to Scheme IV for the generation of *N*-phenylbenzoquinonediimine in the NPA reaction from the corresponding hydroxylamine. However, this mechanism can be ruled out for the reason that the observed rates of reaction at high pH (viz., Figure 3) would require a rate constant of protonation by H_3O^+ that exceeds the diffusion limit by 1 order of magnitude (Eigen & Hammes, 1963). Nevertheless, alternative mechanistic proposals for a nonenzymatic elimination of the hydroxyl group for either substrate via mechanisms involving either general acid (buffer ion) catalysis or spontaneous reaction cannot be ruled out.

Scheme IV

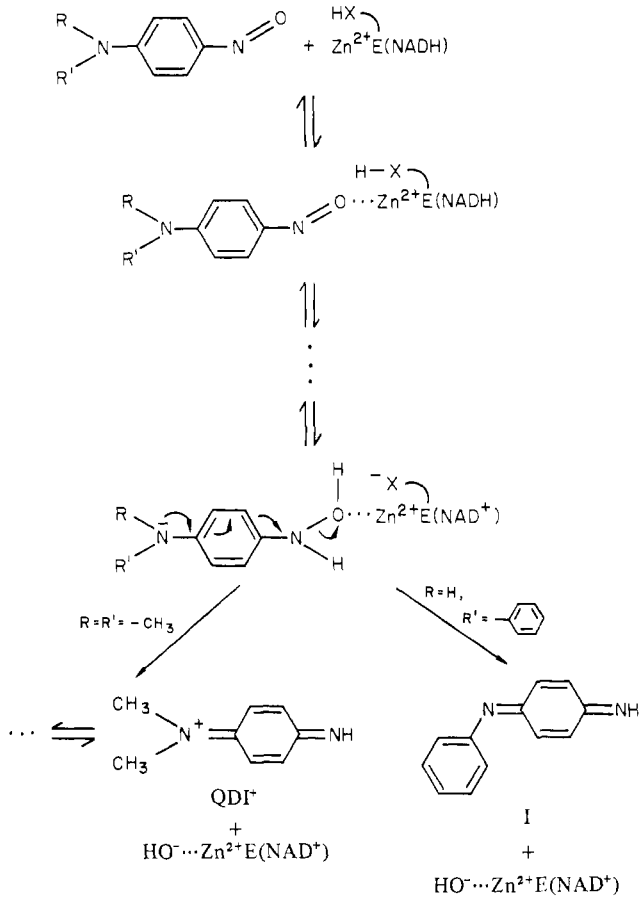

ion to the carbonyl oxygen. Eigen & Wilkins (1964) have proposed that the rate of substitution of inner-sphere water on aquated metal ions by other ligands in nonenzymatic systems is dominated by the dissociation of water. If reaction occurs by a two-step, S_N1-like mechanism for substitution of the zinc-bound water molecule in LADH, then the rates of disappearance of these arylnitroso substrates are limited by the dissociation of the zinc-bound water molecule.

Alternatively, if the zinc ion changes coordination number from a tetracoordinate state in the E(NADH) binary complex to a pentacoordinate state in the E(NADH,S) ternary complex, as was suggested by Dworschack & Plapp (1977), the rate of dissociation of water would not determine the apparent second-order rate constant. Assuming an encounter-controlled limit on the rate of association of RNO with E(NADH), a theoretical upper limit of $\sim 1.5 \times 10^8$ M^{-1} s^{-1} is obtained.[3] Thus, the observed kinetics of the reactions do not a priori preclude a change to pentacoordinate zinc. However, the active-site zinc ion in the 3.7-Å resolution structure of the complex of DACA and 1,4,5,6-tetrahydronicotinamide adenine dinucleotide with LADH appears to be tetrahedral (Brändén et al., 1979; J.-P. Samama and E. Zeppezauer, private communication).

Note that the transient decay of both substrates is independent of pH in the range 4–10 (i.e., when the apparent rate of NPA disappearance is corrected for the ionization of NPA). Also, note that the coordination of the carbonyl oxygen of DACA to the active-site zinc ion of LADH is rapid ($k = 4 \times 10^7$ M^{-1} s^{-1}) and pH independent (Dunn & Hutchinson, 1973; Dunn et al., 1975; Morris et al., 1980). If water dissociation limits the rate of enzyme–substrate combination for both DACA and the nitroso compounds, a decrease in rate would be observed in the pH region of the zinc-bound water pK_a in the E(NADH) complex unless this $pK_a \geq 10$.

If a change in zinc coordination number accompanies substrate coordination, the charge on the putative fourth ligand (i.e., water vs. hydroxide) might be expected to have little influence on the rate of coordination of a neutral fifth ligand (i.e., substrate) with zinc. Alternatively, if substrate binding is a truly diffusion limited process for these nitroso compounds, then the state of ionization of the zinc-coordinated water molecule should have no effect on the observed rates. In this context, it is of interest to compare the E(NADH,S) ternary complex formation rate constants for NDMA, NPA, and DACA with the reaction of benzaldehyde with the E(NADH) complex. The transient kinetic data of Dunn et al. (1979) and Kvassman & Pettersson (1976) suggest the reaction of benzaldehyde with E(NADH) to form the ternary complex occurs with a rate constant $\geq 6 \times 10^6$ M^{-1} s^{-1}, while Weidig et al. (1977) estimate a value of at least 7.7×10^5 M^{-1} s^{-1}. Since these values represent estimated lower limits and are not measured rate constants, it is likely that the actual rate constant is somewhat larger.

The lack of a kinetic isotope effect at pH 7 when NADD is substituted for NADH indicates that hydride transfer is not rate limiting; hence, either dissociation of water or formation of a pentacoordinate zinc ion is a reasonable candidate for the rate-limiting step in the reaction of these substrates with NADH. Since no *enzyme-bound* chemical intermediates are discernible in the conversion of either substrate to the corresponding enzymatic product, the rate(s) of step(s) leading to the loss of the 440-nm absorption for either substrate (i.e., hydride transfer) must be at least comparable to the rate of enzyme–substrate combination. That is, these nitroso substrates undergo a rapid LADH-catalyzed redox–elimination reaction with NADH at a rate which is determined by the formation of the LADH(NADH,S) complex. This is in contrast to the relatively slow rates of reduction of substituted benzaldehydes with electron releasing para substituents. For example, the hydride transfer rate for the LADH-catalyzed reduction of *p*-(*N*,*N*-dimethylamino)benzaldehyde (DMBA) is 0.8 s^{-1} [with 4-hydroxybutyrimidylated enzyme; Dworschack & Plapp (1977)], while *p*-methoxybenzaldehyde exhibits a (saturated) hydride transfer rate of ~ 200 s^{-1} [with native enzyme; Dunn et al. (1979)]. The origins of the extremely large difference in reactivity between NDMA and DMBA are not obvious to us. NDMA is not reduced by $NaBH_4$ in neutral aqueous solution under conditions where DMBA is rapidly reduced.

[3] The theoretical bimolecular rate constant for enzyme–substrate reactions is given by Smoluchowski's equation (Hammes, 1978) as $k = P_1P_2K4\pi aDN_0/1000$, where P_1 and P_2 are probability factors, $K = 1$ for unlike molecules, a is the effective cross section (cm), the diffusion coefficient $D = D_{enzyme} + D_{substrate} \simeq D_{substrate}$ (cm^2 s^{-1}) for small substrates, and N_0 is the Avogadro number. P_1 for LADH is assumed to be the ratio of the area of the active-site cleft opening to the surface area of a sphere with radius equal to the active-site cleft opening to the surface area of a sphere with radius equal to the depth of the active-site cleft. P_2 is the probability of proper orientation of the substrate (assumed to be 1/2 in this case). Assuming the cleft is 20 Å deep, the opening is 100 $Å^2$, $a = 24$ Å, and $D = 8 \times 10^{-6}$ cm^2 s^{-1}, $k = 1.5 \times 10^8$ M^{-1} s^{-1}.

References

Alivisatos, S. G. A., Ungar, F., & Abraham, G. J. (1965) *Biochemistry 4*, 2616.

Anderson, B. M., & Kaplan, N. O. (1959) *J. Biol. Chem. 234*, 1226.

Baetzold, R. C., & Tong, L. K. J. (1971) *J. Am. Chem. Soc. 93*, 1347.

Bamberger, E. (1894) *Chem. Ber. 27*, 1347, 1548.
Brändén, C.-I., Eklund, H., Samama, J.-P., & Wallén, L. (1979) *11th International Congress of Biochemistry*, Toronto, Canada, July 8-13, 1979, Abstr. No. 03-4-S95, p 194.
Cornforth, J. W., Cornforth, R. H., Donninger, C., Popják, G., Ryback, G., & Schroepfer, G. J. (1966) *Proc. R. Soc. London, Ser. B 163*, 436.
DeTraglia, M. C., Schmidt, J., Dunn, M. F., & McFarland, J. T. (1977) *J. Biol. Chem. 252*, 3493.
Dunn, M. F., & Bernhard, S. A. (1971) *Biochemistry 10*, 4569.
Dunn, M. F., & Hutchison, J. S. (1973) *Biochemistry 12*, 4882.
Dunn, M. F., Biellmann, J.-F., & Branlant, G. (1975) *Biochemistry 14*, 3176.
Dunn, M. F., Schack, P., Koerber, S. C., Au, A. M.-J., Saliman, G., & Morris, R. G. (1977) *Pyridine Nucleotide-Dependent Dehydrogenases* (Sund, H., Ed.) pp 206-221, Verlag/W. de Gruyter, New York and Berlin.
Dunn, M. F., Bernhard, S. A., Anderson, D., Copeland, A., Morris, R. G., & Roque, J.-P. (1979) *Biochemistry 18*, 2346.
Dworschack, R. T., & Plapp, B. V. (1977) *Biochemistry 16*, 2716.
Eigen, M., & Hammes, G. G. (1963) *Adv. Enzymol. Relat. Areas Mol. Biol. 25*, 1.
Eigen, M., & Wilkins, R. G. (1964) in *Mechanisms of Inorganic Reactions* (Gould, R. F., Ed.) pp 55-80, American Chemical Society, Washington, DC.
Hammes, G. G. (1978) in *Principles of Chemical Kinetics*, pp 62-67, Academic Press, New York.
Heller, H. E., Hughes, E. D., & Ingold, C. K. (1951) *Nature (London) 168*, 909.
Kvassman, J., & Pettersson, G. (1976) *Eur. J. Biochem. 69*, 279.
McFarland, J. T., & Bernhard, S. A. (1972) *Biochemistry 11*, 1486.
Michaelis, L., Schubert, M. P., & Granick, S. (1939) *J. Am. Chem. Soc. 61*, 1981.
Morris, R. G., Saliman, G., & Dunn, M. F. (1980) *Biochemistry* (second paper of three in this issue).
Plapp, B. V., Eklund, H., & Brändén, C.-I. (1978) *J. Mol. Biol. 122*, 23.
Rafter, G. W., & Colwick, S. P. (1957) *Methods Enzymol. 3*, 887.
Schack, P., & Dunn, M. F. (1972) paper presented at the 8th Federation of European Biochemical Societies Meeting, Amsterdam, Holland, Aug 20-25, 1972.
Shriner, R. L., Fuson, R. C., & Curtin, D. Y. (1959) in *The Systematic Identification of Organic Compounds*, 4th ed., p 162, New York.
Sund, H., & Theorell, H. (1963) *Enzymes, 2nd Ed. 7*, 25.
Theorell, H., & Yonetani, T. (1963) *Biochem. Z. 338*, 537.
Tong, L. K. J., & Glesmann, M. C. (1957) *J. Am. Chem. Soc. 79*, 583.
Weidig, C. F., Halvorson, H. R., & Shore, J. D. (1977) *Biochemistry 16*, 2916.

Phosphoglycerate Mutases: Stereochemical Course of the Phosphoryl Group Transfers Catalyzed by the Cofactor-Dependent Enzyme from Rabbit Muscle and the Cofactor-Independent Enzyme from Wheat Germ†

Walter A. Blättler and Jeremy R. Knowles*

ABSTRACT: 2-[(*R*)-^{16}O,^{17}O,^{18}O]Phospho-D-glycerate has been synthesized and used to determine the stereochemical course of each of the two mechanistic classes of phosphoglycerate mutases. The enzyme from rabbit muscle requires 2,3-bisphospho-D-glycerate as a cofactor and catalyzes an *inter*molecular phosphoryl group transfer reaction. The enzyme from wheat germ requires no cofactor and catalyzes an *intra*molecular transfer of the phosphoryl group. We have shown that the reaction catalyzed by each of these enzymes proceeds with overall *retention* of the configuration at phosphorus. This stereochemical result is consistent with a double-displacement pathway involving a single phosphorylenzyme, for each of the catalyzed reactions.

Phosphoglycerate mutase catalyzes the interconversion of 2- and 3-phospho-D-glycerate, and two classes of enzymes can be distinguished mechanistically. The mutases from animal sources and from yeast show an absolute requirement for the cofactor 2,3-bisphospho-D-glycerate, and these enzymes catalyze the *inter*molecular transfer of phosphoryl groups amongst the two substrates and the cofactor. This class of mutases has been shown to form a chemically competent phosphorylenzyme, the phosphoryl group of which may be transferred to 2-phospho-D-glycerate or 3-phospho-D-glycerate or (much more slowly) to water. It appears that the cofactor 2,3-bisphospho-D-glycerate is required to maintain the enzyme in its active phosphorylated form.

In contrast to the animal and yeast enzymes, the phosphoglycerate mutases from wheat germ and rice germ show no cofactor dependence, and we have shown earlier that the phosphoryl group is transferred *intra*molecularly by the wheat germ enzyme. While for this enzyme no direct evidence could be obtained to demonstrate the intermediacy of a phosphorylenzyme, the behavior of a number of substrate analogues strongly suggested a pathway involving such a species.

† From the Department of Chemistry, Harvard University, Cambridge, Massachusetts 02138. *Received August 24, 1979.* This work was supported by a fellowship from the Schweizerische Nationalfond (W.A.B.) and by the National Institutes of Health.

0006-2960/80/0419-0738$01.00/0